

Contact Angle of Liquid ^4He on a Cs Surface

J. Klier, P. Stefanyi, and A. F. G. Wyatt

Department of Physics, University of Exeter, Stocker Road, Exeter, EX4 4QL, Devon, United Kingdom
(Received 14 August 1995)

We have measured the contact angle Θ of ^4He on cesium-coated tungsten plates as a function of temperature. We find that Θ decreases to zero at $T \approx 2.0$ K in agreement with the wetting temperature found on bulk Cs. At $T = 0$ K the contact angle is $48^\circ \pm 1^\circ$, significantly larger than the predicted value of approximately 30° . The energy of the interface between Cs and liquid ^4He has a large temperature dependence. This suggests that there are low-lying excitations on the liquid helium surface at this interface. Indeed it appears that liquid ^4He at this interface is similar to that at a free surface.

PACS numbers: 67.70.+n, 68.10.Cr, 68.45.Gd

Liquid ^4He wets most materials and was thought until recently to be a universal wetting liquid. However, theoretical calculations [1,2] have predicted that ^4He will not wet some alkali metals below a certain temperature called the wetting temperature T_w . Subsequent experiments have indeed shown that ^4He does not wet Cs [3–5] and Rb [6]. This has been demonstrated by showing that the adsorbed helium film on Cs or Rb for $T < T_w$ is atomically thin and only becomes macroscopically thick for $T > T_w$. This arises from the fact that the substrate surface is always attractive to ^4He , but, if it is less attractive than the liquid-liquid attraction, then only a few atomic layers of ^4He at most can form at $T < T_w$. This thin film can disappear as $T \rightarrow 0$ as found for Cs [5].

Another important property of a liquid that does not wet a substrate is that it forms drops of macroscopic size with a finite contact angle Θ . This angle is in general temperature dependent for $T < T_w$ and goes to zero at T_w and remains zero at all higher temperatures where the liquid wets the substrate. In fact, a nonzero contact angle is the usual indication of nonwetting, for example, water drops on solid hydrocarbons and mercury on glass.

Besides this visual indication of wetting and nonwetting, the contact angle has an important connection to the free energies of the three interfaces involved. These are σ_{lv} , σ_{sv} , and σ_{sl} , which are, respectively, between liquid-vapor, substrate-vapor, and substrate-liquid. Young's equation connects these to Θ as

$$\cos\Theta = \frac{\sigma_{sv} - \sigma_{sl}}{\sigma_{lv}}. \quad (1)$$

While σ_{lv} can be readily measured and is indeed well known for ^4He [7], the other interface free energies are not known, and so a measurement of $\Theta(T)$ allows $\sigma_{sv} - \sigma_{sl} \equiv \Delta\sigma$ to be determined and deductions to be made for σ_{sv} and σ_{sl} .

The first theoretical estimate for $\Theta(0)$ for ^4He on Cs was $\approx 95^\circ$ [1]. This was revised to $\approx 30^\circ$ [8] when T_w was measured to be ≈ 2 K [3,4], which was half that estimated theoretically. These estimates were based on the assumption that $\Delta\sigma$ was temperature independent so

that $\Theta(0)$ is given by $\cos\Theta(0) = \Delta\sigma/\sigma_{lv}(0)$ with $\Delta\sigma = \sigma_{lv}(T_w)$. Since then there have been calculations of the temperature dependence of $\Delta\sigma$ [9], especially σ_{sl} , which show that it is rather small compared to that of $\sigma_{lv}(T)$, and so the assumption above appears to be a good first approximation. However, there is recent experimental evidence that σ_{sl} is a strong function of temperature and that the Cs-helium interface resembles the free liquid surface [10].

We report here the first measurement of the contact angle for ^4He on Cs and its temperature dependence. We find that the contact angle is much larger than expected and this has important implications for the liquid ^4He -Cs interface.

We choose to measure the contact angle from the force created in a capillary formed by two parallel plates. Consider the space between two vertical plates of horizontal length l and separated by a distance d containing liquid ^4He . The upward force per unit length on the liquid due to one plate is $\sigma_{lv} \cos\Theta$, which gives a pressure reduction in the liquid due to both plates of $2\sigma_{lv} \cos\Theta/d$ [when plates have vertical spacers at the edges, this equation becomes $2(l+d)\sigma_{lv} \cos\Theta/ld$]. We measure this decrease in pressure with a pressure gauge at the bottom of the column of liquid ^4He into which the plates are dipping at the liquid-vapor interface. The arrangement is shown in the inset of Fig. 2.

The stainless steel cell contains an array of equally spaced W plates. The base of the cell is connected to the capacitive pressure gauge. The connecting tube contains a breakable seal that is broken only at $T \approx 2.2$ K, so that the Cs-coated plates are not connected to the pressure gauge during their preparation. This is because the pressure gauge can neither be exposed to Cs nor have an ultrahigh vacuum (UHV) inside it at room temperature. Helium is added to both sides of the flexible capacitance diaphragm through valves that can be closed at low temperature to superfluid tightness. The whole system is in a bath of superfluid ^4He , which provides a constant temperature enclosure. The temperature is measured with a calibrated Ge thermometer [11].

The cell housing the plates is made of stainless steel and sealed with UHV flanges and copper gaskets to enable it to be pumped and baked to high vacuum conditions before the plates are coated with Cs. We use tungsten plates as it is known that a Cs film will form on a tungsten surface, especially if it is a slightly oxidized surface [12]. There are 254 plates 100 μm thick and separated by $d = 100 \mu\text{m}$. Each plate side has a contact length $l = 16 \text{ mm}$ with the liquid. The principal reason for using many plates is that the liquid level must not change too much during a temperature scan.

The flexible diaphragm of the pressure gauge is made of a 12 μm thick Mylar foil aluminized on one side. This diaphragm is sealed at the edges so that there is no superfluid connection across it. The lower half of the pressure gauge is partially filled by liquid ^4He , which ensures that the pressure due to the vapor on each side of the diaphragm is equal. Purified ^4He is used both above and below the diaphragm [13]. The capacitance between the metalized diaphragm and the flat counter electrode is measured with a capacitance bridge. The reference capacitor of 10^3 pF is in a screened box in the helium bath at 4.2 K.

The preparation of the Cs-coated plates is done at room temperature and above. Before the coating process the plates are cleaned with dilute sodium hydroxide and then assemble in the cell. After the cell is closed a break-seal Cs ampoule (purity is 99.98%, Alpha Chemicals) is attached via a glass-to-metal seal and the whole assembly pumped and baked at 200 $^\circ\text{C}$ for several days until a pressure less than 10^{-7} mbar is reached. Then the break seal on the ampoule is broken and a small amount of molten Cs transferred close to the cell. The ampoule is then detached from the cell and the actual evaporation and coating process started. After maintaining the Cs and the cell at 200 $^\circ\text{C}$ for several hours (the vapor pressure of Cs is about 0.1 mbar at this temperature) the cell is slowly and steadily cooled. The necessity of the slow cooling process is to get an even coat of Cs on all plates by avoiding preferential condensation of Cs on the walls of the cell, which are necessarily colder. After the cell has reached room temperature it is connected to the pressure gauge and then mounted inside a vessel, which is then anchored to a dilution refrigerator. At low temperatures, this vessel is filled with liquid helium to avoid temperature gradients between the cell and the pressure gauge as we vary the temperature from 60 mK up to T_λ .

The stability of the pressure gauge is measured with no helium on either side of the diaphragm. Over the entire temperature region ($60 \text{ mK} < T < 2.2 \text{ K}$) the fractional change in capacitance is less than 10^{-6} , and the random noise and stability is an order of magnitude less. The pressure gauge is then calibrated using saturated vapor pressure of a small amount of ^4He above the diaphragm up to 1.58 K (the saturated vapor pressure at 1.41 K corresponds to the maximum capacitance during the experi-

ment, $\approx 1000 \text{ pF}$). From this the capacitance-pressure relationship is determined.

There are three effects that change the pressure in a temperature scan besides the temperature dependence of Θ and σ_{lv} . The first is due to the temperature dependence of the liquid density, which would not change the pressure if the liquid container had a uniform cross section. But with our arrangement of two chambers connected by a tube, if the liquid expands then the pressure rises. This effect can be calculated from the geometry of the apparatus and the measured values of $\rho_{\text{liq}}(T)$ [14]. The second effect is due to the ratio of liquid to vapor in the fixed mass of helium in the column above the diaphragm. The amount of liquid decreases as the temperature is raised due to evaporation, and so this leads to a decrease in pressure. Again this can be calculated from density of the vapor $\rho_{\text{vap}}(T)$ and $\rho_{\text{liq}}(T)$ together with the geometry.

The third effect is smaller and more subtle. Below the diaphragm the space between the diaphragm and the fixed electrode is filled with liquid helium by capillary condensation. The free liquid surface is 27 mm below the diaphragm. The pressure in liquid helium in contact with the diaphragm is lower than the vapor pressure by $\rho_{\text{liq}}gh$, where h is the vertical distance between the diaphragm and the free liquid surface below it. Also the liquid ^4He between the capacitor plates has a small temperature dependent dielectric constant. The measured capacitances are corrected for this dielectric change before they are converted into pressure. The values for $\epsilon_r(T)$ are taken from [14].

To check that we understood our apparatus and these contributions to the temperature dependent pressure, we established the liquid level just below the vertical plates. At this position the surface tension makes a negligible contribution to the pressure. The calculated contributions to the pressure change with temperature are shown in the inset of Fig. 1. The measured capacitance together with the calculated values as a function of temperature up to T_λ are shown in Fig. 1. With the excellent correspondence between the measured and calculated pressure changes, we then set the liquid level within the Cs-coated plates and measured the pressure change with temperature. The temperature scans were made very slowly; the warming took seven days and the cooling about four days. There is a noticeable difference between warming and cooling with the cooling data falling below the warming data; see Fig. 2. This hysteresis is probably due to the difference in the advancing and receding contact angle and a nucleation barrier near T_w . We subtract the three contributions discussed above and so obtain $\sigma_{lv} \cos\Theta$. Then using the measured temperature dependence of σ_{lv} we obtain $\Theta(T)$, which is shown in Fig. 3. We find $\Theta(0) = 48^\circ \pm 1^\circ$ and $T_w = 2.0 \pm 0.05 \text{ K}$.

Having obtained $\Theta(T)$, we now explore the consequences of Young's equation. In Fig. 4 we show the surface free energies σ_{lv} and $\Delta\sigma = \sigma_{sv} - \sigma_{sl}$. The value

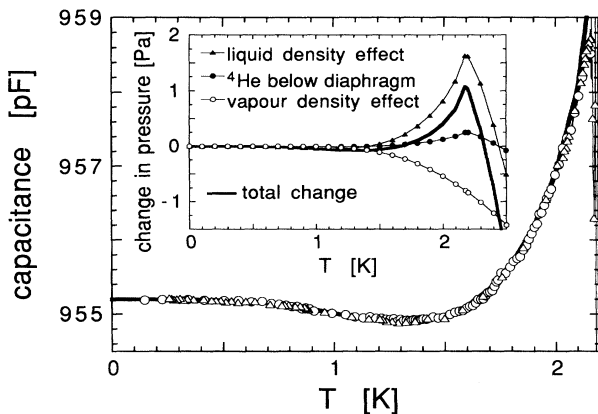


FIG. 1. The change in capacitance with temperature with the liquid ⁴He level just below the Cs-coated plates is compared with calculated values (solid line). Every tenth data point is plotted. The inset shows the different effects that change the pressure, as described in the text. The total contribution is shown as the solid line. There are no free parameters in this model, which gives very good agreement with the measurements.

of $\Delta\sigma$ is calculated from the contact angle data in Fig. 3 together with $\sigma_{lv}(T)$ [7] using Eq. (1). It is worth noting that we need only the temperature dependence of σ_{lv} and not its value at $T = 0$ K. The hysteresis in the contact

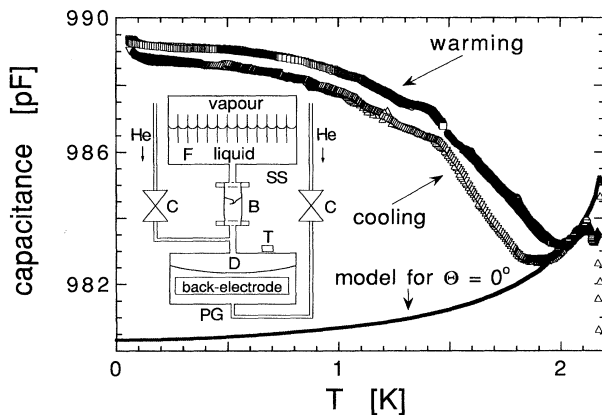


FIG. 2. The measured capacitance as a function of temperature with the helium level within the Cs-coated plates. The upper curve shows two temperature scans from low to high temperature, whereas the lower one shows two cooling scans. The solid line is the calculated capacitance with $\Theta = 0^\circ$. The wetting temperature is where this line intersects the measured line and is clearly less than T_λ . Inset: The schematic drawing of the experimental setup. The top part shows the stainless steel cell (SS) with the Cs-coated W plates (F). In the middle is the breakable seal (B), which joins the upper cell to the pressure gauge (PG) with diaphragm (D). The filling lines to the upper and lower part of the pressure gauge can be closed by superfluid-tight needle valves (C). The Ge thermometer (T) is located on top of the pressure gauge. The whole is immersed in superfluid ⁴He.

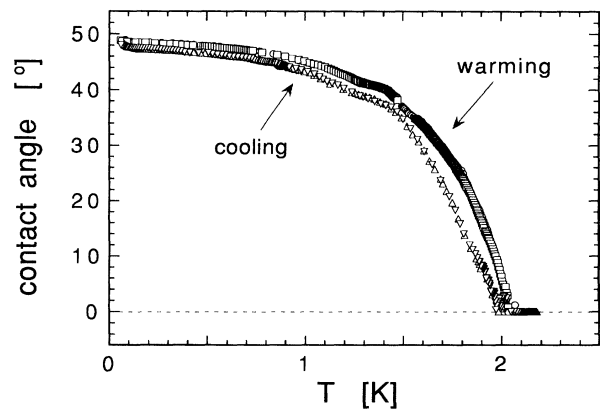


FIG. 3. The contact angle is shown as a function of temperature. It is determined from the difference in the data points and the model for $\Theta = 0^\circ$ in Fig. 2. Every fifth data point is plotted. Again the upper curve stems from warming and the lower one from cooling.

angle separates the two data sets in Fig. 4. The surprise from these measurements is the large change in $\Delta\sigma$ with temperature. It is indeed larger than the change in σ_{lv} .

The main temperature dependence of $\Delta\sigma$ is likely to come from σ_{sl} because σ_{sv} is, to a first approximation, equal to the surface energy of the bare Cs surface, $\sigma_{s,vac}$. The next approximation is to consider the thin layer of He on the Cs, i.e., $\sigma_{sv} \approx \sigma_{s,vac} + \sigma_{He \text{ layer}}$. If we model this He layer as a 2D gas we find that $\sigma_{He \text{ layer}}$, for one monolayer, changes between 0 and 2 K by an amount that is an order of magnitude less than that for σ_{lv} . Also the change is negative, which is in the opposite direction to the change in $\Delta\sigma$ that we measure. It is possible that close to T_w the thin He layer becomes a 2D liquid. In general we can argue that such a layer would have thermal

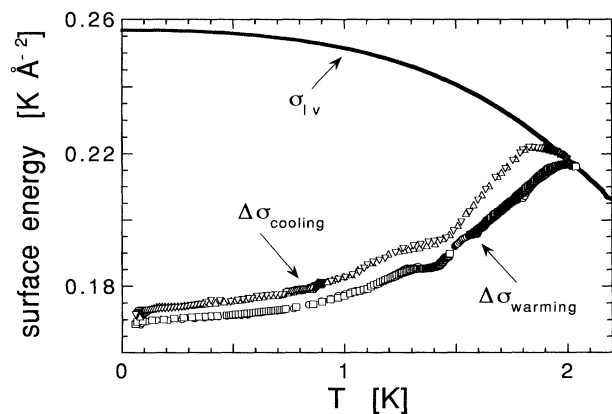


FIG. 4. The surface free energy difference $\Delta\sigma = \sigma_{sv} - \sigma_{sl}$ is shown as a function of temperature together with $\sigma_{lv}(T)$ [7]. The data sets come from the two cooling and the two warming scans (every fifth data point is plotted).

excitations that again would lower the surface free energy as the temperature increases. Because of the thinness of any such liquid He film (of the order of 1 atomic layer), these excitations would have a higher velocity than those on the free liquid surface [15], so the change in $\sigma_{\text{He layer}}$ would be small compared to the change in σ_{lv} over the same temperature interval.

From the above discussion we do not consider that $\sigma_{sv}(T)$ is the cause of the measured temperature dependence of $\Delta\sigma$, so we now examine $\sigma_{sl}(T)$. We can write this as $\sigma_{sl}(T) \approx \sigma_{s,\text{vac}} + \sigma_{l,\text{Cs}} + \int \rho V dz$ [16], where $\sigma_{l,\text{Cs}}$ is the free energy of the surface of the liquid ^4He at the liquid-Cs interface and $\int \rho V dz$ is due to the van der Waals attraction between ^4He and Cs. The only term that is significantly dependent on temperature is $\sigma_{l,\text{Cs}}$. This temperature dependence term has been calculated [9] and found to be $-7 \times 10^{-4} T^3 \text{ K } \text{\AA}^{-2}$. The reason for this is that the excitations of the liquid surface at the Cs boundary have a nearly linear dispersion with a velocity comparable to the bulk phonons, whereas at the free surface there are the much lower-frequency ripples. Presumably this difference is due to the Cs suppressing displacements of the liquid in the direction of the normal to the surface. Our results in Fig. 4 show a much larger change with temperature than this calculation predicts. Also, our values for $\sigma_{l,\text{Cs}}(T)$ are approximately twice as large than those estimated from the wetting temperature of He on Cs-coated Au [10]. However, these estimates depend strongly on the assumption that $\sigma_{l,\text{Cs}}(0) = \sigma_{lv}(0)$.

Summarizing this discussion, we think it is unlikely that the considerable temperature dependence of $\Delta\sigma$ is due to $\sigma_{sv}(T)$ as the expected change with temperature is too small and in the wrong direction. Although the calculated change in σ_{sl} is in the right direction, it is again too small [9]. However, if we take the liquid ^4He against the Cs to be a free liquid surface, then we get the right magnitude of temperature dependence, which suggests that there are low energy excitations at this surface as on the free liquid surface.

In conclusion, we have measured the contact angle of liquid ^4He on Cs as a function of temperature from $T \ll T_w$ to $T_w = 2 \text{ K}$. We have used Cs-coated W plates, which give the same T_w as found by others with bulk Cs [3] and evaporated Cs films [4]. The contact

angle is finite for $T < T_w$ and goes to zero at T_w as expected. The contact angle of 48° as $T/T_w \rightarrow 0$ is much larger than expected, and correspondingly the temperature dependence of the free energy of the Cs-liquid ^4He interface is also large. We have argued that this is because the surface of the liquid ^4He at the Cs boundary behaves as though it is essentially free. This is contrary to current theories and suggests that there are low energy excitations at this interface that have not yet been considered.

The authors wish to thank E. Lammers for her help with the development of data acquisition software for the measurements.

-
- [1] E. Cheng, M. W. Cole, W. F. Saam, and J. Treiner, *Phys. Rev. Lett.* **67**, 1007 (1991).
 - [2] E. Cheng, M. W. Cole, W. F. Saam, and J. Treiner, *Phys. Rev. B* **46**, 13967 (1992).
 - [3] P. J. Nacher and J. Dupont-Roc, *Phys. Rev. Lett.* **67**, 2966 (1991).
 - [4] J. E. Rutledge and P. Taborek, *Phys. Rev. Lett.* **69**, 937 (1992); **71**, 263 (1993).
 - [5] P. Stefanyi, J. Klier, and A. F. G. Wyatt, *Phys. Rev. Lett.* **73**, 692 (1994).
 - [6] A. F. G. Wyatt, J. Klier, and P. Stefanyi, *Phys. Rev. Lett.* **74**, 1151 (1995).
 - [7] M. Iino, M. Suzuki, and A. J. Ikushima, *Can. J. Phys.* **65**, 155 (1986).
 - [8] M. S. Petterson and W. F. Saam, *J. Low Temp. Phys.* **90**, 159 (1993).
 - [9] L. Pricaupenko and J. Treiner, *J. Low Temp. Phys.* **96**, 19 (1994).
 - [10] D. Ross, P. Taborek, and J. E. Rutledge, *Phys. Rev. Lett.* **74**, 4483 (1995).
 - [11] Lake Shore Cryotronics, Inc., Model GR-200A-30.
 - [12] C. C. Addison, *Chemistry of Alkali Metals* (Wiley, New York, 1985).
 - [13] Isotopically purified ^4He supplied by P. V. C. McClintock, University of Lancaster.
 - [14] J. J. Niemela and R. J. Donnelly, *J. Low Temp. Phys.* **98**, 1 (1995).
 - [15] B. E. Clements, H. Forbert, E. Krotscheck, and M. Saarela, *J. Low Temp. Phys.* **95**, 849 (1994).
 - [16] E. Cheng, M. W. Cole, J. Dupont-Roc, W. F. Saam, and J. Treiner, *Rev. Mod. Phys.* **65**, 557 (1993).